

“Direct” Calculation of Thermal Rate Constants for the $F + H_2 \rightarrow HF + H$ Reaction

Haobin Wang, Ward H. Thompson,[†] and William H. Miller*

Department of Chemistry, University of California, and Chemical Sciences Division,
Lawrence Berkeley Laboratory, Berkeley, California 94720

Received: March 11, 1998

We present “direct” calculations of the thermal rate constant for the $F + H_2$ reaction. The rate is obtained from the time integral of the flux–flux autocorrelation function, which is efficiently evaluated by taking advantage of the low rank of the half-Boltzmannized flux operator. Total rate constants are obtained from exact total angular momentum $J \neq 0$ calculations and compared with approximate approaches for including nonzero J . The rate constants obtained for the $F + H_2$ reaction on the new, highly accurate Stark–Werner potential energy surface are in good agreement with previous experimental results.

I. Introduction

A great deal of progress has been made over the last few years in the ability to calculate rate constants for chemical reactions—both canonical (i.e., thermally averaged) and microcanonical—by quantum mechanical methods that are *direct*, i.e., avoid having to solve the state-to-state reactive scattering problem explicitly, yet also *correct*, i.e., in principle exact (for a given potential energy surface); ref 1 reviews this methodology and its recent applications. The approach, which has qualitative vestiges and some of the efficiencies of transition-state theory, involves only the short time quantum dynamics of the system in the transition-state region of the potential surface; one may think of it as the quantum analogue of the procedure in classical mechanics of beginning trajectories on a dividing surface in the transition-state region (with their initial conditions sampled from a Boltzmann distribution) and following them only so long as necessary to see which ones are reactive (i.e., determining the “transmission coefficient”).

The thermal rate constant is obtained in this approach as the time integral of a flux–flux autocorrelation function $C_{ff}(t)$,^{2–4}

$$k(T) = Q_r(T)^{-1} \int_0^\infty dt C_{ff}(t) \quad (1.1)$$

where

$$C_{ff}(t) \equiv \text{tr}[\hat{F}(\beta) e^{i\hat{H}t/\hbar} \hat{F} e^{-i\hat{H}t/\hbar}] \quad (1.2)$$

and $Q_r(T)$ is the reactant partition function per unit volume, \hat{H} is the Hamiltonian operator of the complete molecular system, \hat{F} is the symmetrized flux operator determined with respect to a dividing surface separating reactants and products, $\hat{F}(\beta)$ is the Boltzmannized flux operator,

$$\hat{F}(\beta) \equiv e^{-\beta\hat{H}/2} \hat{F} e^{-\beta\hat{H}/2} \quad (1.3)$$

and $\beta = (k_B T)^{-1}$. The evaluation of the flux correlation function is especially efficient for the case of direct reactions, i.e., those that do not involve the formation of a long-lived collision complex, as has been well demonstrated by applications to the

reactions $D + H_2 \rightarrow DH + H$,⁵ $O + HCl \rightarrow OH + Cl$,⁶ and $Cl + H_2 \rightarrow HCl + H$.⁷

In brief, the efficiency of the overall procedure stems from two features: first, $\hat{F}(\beta)$ is of low rank, i.e., has only a few nonzero eigenfunctions, so they can be obtained extremely efficiently by the Lanczos algorithm;^{8,9} $\hat{F}(\beta)$ is then represented in terms of its eigenvectors $\{|v_m\rangle\}$ and eigenvalues $\{f_m\}$,

$$\hat{F}(\beta) = \sum_m |v_m\rangle f_m \langle v_m| \quad (1.4)$$

so that the trace in eq 1.2 gives the correlation function as

$$C_{ff}(t) = \sum_m f_m \langle v_m(t) | \hat{F} | v_m(t) \rangle \quad (1.5)$$

where $|v_m(t)\rangle$ is the time-evolved flux eigenvector

$$|v_m(t)\rangle = e^{-i\hat{H}t/\hbar} |v_m\rangle \quad (1.6)$$

In the time propagation, eq 1.6, an absorbing potential is added to the Hamiltonian in the usual way^{10–16} to prevent unphysical reflection from the edge of the grid or other finite basis representation of \hat{H} . For the applications noted above, the basis set used to represent the Hamiltonian ranged from ~ 700 to $\sim 20\,000$, yet the rank of $\hat{F}(\beta)$ was only ~ 12 and ~ 40 , respectively; it is only these relatively few vectors that must be time-evolved (cf. eq 1.6). Furthermore, for direct reactions only short time evolution is required, a time of $\sim \hbar\beta$ (which is 27 fs for $T = 300$ K), and this is the second feature that leads to the efficiency of the overall procedure. In the language of transition-state theory, step 1—the Lanczos procedure to obtain the eigenvectors and eigenvalues of $\hat{F}(\beta)$ —may be thought of as “finding the states of the activated complex”, and step 2—the time evolution of the eigenvectors—as “determining the transmission coefficient” for each of these states. The approach is exact, however, and thus also applicable to nondirect, i.e., complex-forming, reactions, such as¹⁷



but long time evolution is required, e.g., ~ 1 ps for the $H + O_2$ reaction. Finally, it should be noted that the approach summarized above has some significant features in common with

[†] Current address: Department of Chemistry and Biochemistry, University of Colorado, Boulder, CO 80309.

* Corresponding author.

the excellent work of Light and co-workers¹⁸ and that of Manthe¹⁹ on this general topic, though there are also significant differences.

This paper presents the results of such calculations of the thermal rate constant for the much studied $F + H_2 \rightarrow HF + H$ reaction using the most recently, and presumably most accurate, ab initio potential energy surface available, that of Stark and Werner.²⁰ The $F + H_2$ reaction has long served as a benchmark for atom–diatom scattering and has attracted a great deal of interest in the past few years. In particular, recent experimental measurements of the FH_2^- photodetachment spectra to probe the $F + H_2$ transition-state region,²¹ combined with theoretical simulations,²² have established that the transition state has a bent geometry.²³ This reaction is also significantly different from the others noted above in that, though it is basically a direct reaction, it has a very low barrier and is very exothermic. These features have caused us to modify somewhat the procedure summarized above, as is described in section II. The specifics of the calculation, e.g., exact and approximate ways of treating total angular momentum $J > 0$, are described in section III, and the results are presented and discussed in section IV.

II. Theory

In attempting to apply the approach summarized in the Introduction to the $F + H_2$ reaction at low temperature (even 300 K), the imaginary time $\hbar\beta$ is sufficiently large that problems arise in constructing the eigenvalues/vectors of the Boltzmannized flux operator of eq 1.3. This is because the Boltzmann operator is diffusive in character, and the strongly exothermic region of the potential energy surface in the product ($HF + H$) region tends to localize the eigenvectors $\{|v_m\rangle\}$ in that region. This then leads to large recrossing contributions to the flux correlation function, i.e., negative values of $C_{ff}(t)$, the integral of which leads to large cancellation of the positive contribution; cf. the classical simulation, where most trajectories that are begun in the $HF + H$ region will not go to $F + H_2$. This can be partially remedied by locating the dividing surface farther out in the reactant ($F + H_2$) region, but this then requires longer propagation times.

The most useful way we have found for overcoming this problem has been to make the imaginary (diffusive) time shorter by employing a variant of the formulation used earlier (for other reasons) by Park, Brown, and Light:¹⁸ note that since the Boltzmann operator and time evolution operator commute, eq 1.2 can be written in the equivalent form

$$C_{ff}(t) = \text{tr}[e^{-\beta\hat{H}/4}\hat{F}e^{-\beta\hat{H}/4}e^{i\hat{H}t/\hbar}e^{-\beta\hat{H}/4}\hat{F}e^{-\beta\hat{H}/4}e^{-i\hat{H}t/\hbar}] \\ \equiv \text{tr}[\hat{F}(\beta/2)e^{i\hat{H}t/\hbar}\hat{F}(\beta/2)e^{-i\hat{H}t/\hbar}] \quad (2.1)$$

where $\hat{F}(\beta/2)$ is the “half-Boltzmannized” flux operator

$$\hat{F}(\beta/2) = e^{-\beta\hat{H}/4}\hat{F}e^{-\beta\hat{H}/4} \quad (2.2)$$

which is also of low rank. The Lanczos algorithm is used as before to find the nonzero eigenvalues and corresponding eigenvectors of $\hat{F}(\beta/2)$, which we denote here as $\{f_m\}$ and $\{|v_m\rangle\}$ (and trust they will not be confused with the eigenvalues/vectors of $\hat{F}(\beta)$ in the Introduction). $\hat{F}(\beta/2)$ is then represented as

$$\hat{F}(\beta/2) = \sum_m |v_m\rangle f_m \langle v_m| \quad (2.3)$$

and this expansion is used for both operators $\hat{F}(\beta/2)$ in eq 2.1,

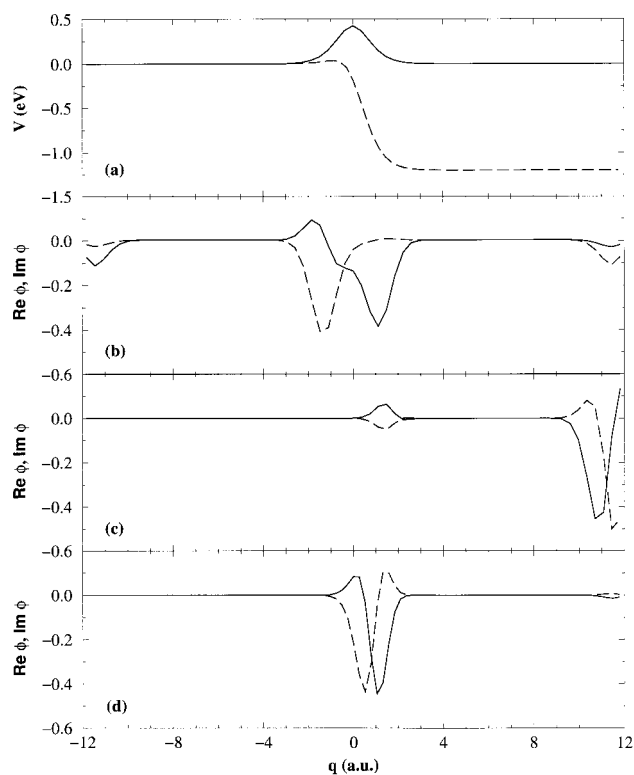


Figure 1. (a) Symmetric (solid line) and asymmetric (dashed line) Eckart barrier potentials. Eigenvector corresponding to the largest eigenvalue of the Boltzmannized flux operator at $T = 300$ K is shown for the symmetric Eckart barrier (b) and for the asymmetric Eckart barrier (c). The real part is given by the solid line and the imaginary part by the dashed line. (d) Analogous eigenvector at $T = 600$ K for the asymmetric Eckart barrier.

which gives the trace as

$$C_{ff}(t) = \sum_{m,m'} f_m f_{m'} \langle v_m | e^{i\hat{H}t/\hbar} | v_{m'} \rangle \langle v_{m'} | e^{-i\hat{H}t/\hbar} | v_m \rangle \\ = \sum_{m,m'} f_m f_{m'} |\langle v_{m'} | v_m(t) \rangle|^2 \quad (2.4)$$

where $|v_m(t)\rangle$ is the time-evolved vector

$$|v_m(t)\rangle = e^{-i\hat{H}t/\hbar} |v_m\rangle \quad (2.5)$$

The primary advantage of this version of the calculation is that the eigenvectors of $\hat{F}(\beta/2)$ have only half as long in imaginary time to diffuse away from the dividing surface as do the eigenvectors of $\hat{F}(\beta)$. The dramatic effect this can have is illustrated in Figure 1 for a one-dimensional Eckart potential. Figure 1a shows the potential for a symmetric reaction, such as $H + H_2 \rightarrow H_2 + H$, and also for a strongly asymmetric one corresponding approximately to $F + H_2 \rightarrow HF + H$. Figure 1b shows the real and imaginary parts of the eigenvector²⁴ of $\hat{F}(\beta)$ at $T = 300$ K for the symmetric case; the eigenvector is localized about the dividing surface (located in all cases at the top of the barrier), with small peaks at the edge of the grid. Figure 1c shows how different things are for the asymmetric case, where the eigenvector has diffused far away from the dividing surface into the exothermic region. Figure 1d shows the eigenvector for the asymmetric case for $T = 600$ K, corresponding to $\beta \rightarrow \beta/2$, and one sees that it is still very much localized about the dividing surface. The eigenvectors of $\hat{F}(\beta/2)$ are thus much more localized about a dividing surface through

the transition-state region than those of $\hat{F}(\beta)$, which is precisely what we hoped to achieve.

There is, moreover, another bonus that one achieves by utilizing both the formulation in the Introduction, eqs 1.2–1.6, and the above variation, eqs 2.1–2.5, because the eigenvalues and eigenvectors of $\hat{F}(\beta/2)$ for temperature T are those of $\hat{F}(\beta)$ for temperature $2T$. Thus the eigenvalues $\{f_m\}$ and eigenvectors $\{|v_m\rangle\}$ of $\hat{F}(\beta/2)$ used to construct the flux correlation function at temperature T via eq 2.4, i.e.,

$$C_T(t) = \sum_{m,m'} f_m f_{m'} |\langle v_{m'} | v_m(t) \rangle|^2 \quad (2.6a)$$

can also be used in eq 1.5 to obtain the flux correlation function at temperature $2T$,

$$C_{2T}(t) = \sum_m f_m \langle v_m(t) | \hat{F} | v_m(t) \rangle \quad (2.6b)$$

Therefore with one Boltzmannized flux eigenvalue/vector calculation and one time evolution of these eigenvectors, one is able to obtain the rate constants at T and $2T$! [One may, though, need more terms to achieve convergence for the higher temperature, eq 2.6b, than for the lower temperature because the contribution from the smaller eigenvalues dies off only as $O(f)$ in eq 2.6b but as $O(f^2)$ in eq 2.6a.]

III. Details of Calculation

A. Coordinate System and Hamiltonian. The coordinates and form of the Hamiltonian are essentially identical to those used before in our $\text{Cl} + \text{H}_2 \rightarrow \text{HCl} + \text{H}$ paper.⁷ Thus we have used the standard Jacobi coordinates of the $\text{F} + \text{H}_2$ arrangement: r is the H–H bond distance, R the distance from F to the center-of-mass of H_2 , and γ the angle between \mathbf{r} and \mathbf{R} . In terms of them, the total Hamiltonian in the body-fixed frame can be written as²⁵

$$\hat{H} = \hat{T}_R + \hat{T}_r + \left(\frac{1}{2\mu R^2} + \frac{1}{2mr^2} \right) \hat{j}^2 + \frac{1}{2\mu R^2} (\hat{J}^2 - 2\hat{J}_z^2 + \hat{A} + \hat{B}) + \hat{V}(R, r, \gamma) \quad (3.1a)$$

where

$$\hat{T}_R = -\frac{\hbar^2}{2\mu} \frac{\partial^2}{\partial R^2} \quad (3.1b)$$

$$\hat{T}_r = -\frac{\hbar^2}{2m} \frac{\partial^2}{\partial r^2} \quad (3.1c)$$

$$\hat{j}^2 = -\hbar^2 \left(\frac{\partial^2}{\partial \gamma^2} + \cot \gamma \frac{\partial}{\partial \gamma} - \frac{1}{\hbar^2 \sin^2 \gamma} \hat{J}_z^2 \right) \quad (3.1d)$$

$$\hat{A} = \hat{J}_+ \left(\hbar \frac{\partial}{\partial \gamma} - \cot \gamma \hat{J}_z \right) \quad (3.1e)$$

$$\hat{B} = \hat{J}_- \left(-\hbar \frac{\partial}{\partial \gamma} - \cot \gamma \hat{J}_z \right) \quad (3.1f)$$

Here μ is the reduced mass of F and H_2 , and m that of the two H atoms. \hat{J}^2 is the total angular momentum operator, \hat{J}_z is the projection operator of total angular momentum along the body-

fixed axis (\mathbf{R}), and \hat{J}_+ and \hat{J}_- are raising and lowering operators. These operators satisfy

$$\hat{J}^2 (D_{MK}^J)^* = \hbar^2 J(J+1) (D_{MK}^J)^* \quad (3.2a)$$

$$\hat{J}_z (D_{MK}^J)^* = \hbar K (D_{MK}^J)^* \quad (3.2b)$$

$$\hat{J}_\pm (D_{MK}^J)^* = \hbar \Lambda_{JK}^\pm (D_{MK\pm 1}^J)^* \quad (3.2c)$$

and

$$\Lambda_{JK}^\pm = \sqrt{J(J+1) - K(K\pm 1)} \quad (3.2d)$$

where D_{MK}^J is the usual Wigner function,²⁶ J the total angular momentum quantum number, M the projection of total angular momentum onto the space-fixed axis, and K its projection onto the body-fixed axis (\mathbf{R}).

Choosing the basis functions as a set of symmetrized Wigner functions

$$|JMK; \sigma\rangle \equiv \frac{1}{\sqrt{2(1+\delta_{K0})}} [D_{MK}^J + (-1)^{J+K+\sigma} D_{M-K}^J]^* \quad (3.3)$$

where $\sigma = 0$ or 1 is the parity index for the total space inversion, the matrix of \hat{H} with respect to this basis is diagonal in J , M , and σ (and in fact independent of M), but not in K .²⁷

$$\begin{aligned} \langle JMK'; \sigma | \hat{H} | JMK; \sigma \rangle &\equiv H_{K',K}^{J,\sigma} \\ &= \delta_{K',K} \left\{ \hat{T}_R + \hat{T}_r + \hat{T}_\gamma + \hat{V}(R, r, \gamma) + \right. \\ &\quad \left. \frac{\hbar^2}{2\mu R^2} [J(J+1) - 2K^2] \right\} - \\ &\quad \frac{\hbar}{2\mu R^2} (\delta_{K',K+1} \sqrt{1+\delta_{K,0}} \Lambda_{JK}^+ \hat{J}_+ + \delta_{K',K-1} \sqrt{1+\delta_{K,1}} \Lambda_{JK}^- \hat{J}_-) \end{aligned} \quad (3.4a)$$

where

$$\hat{T}_\gamma = \left(\frac{1}{2\mu R^2} + \frac{1}{2mr^2} \right) \hat{j}^2 \quad (3.4b)$$

The parity σ determines the range of K and K' , i.e. when $J + \sigma$ is even, $K, K' = 0, \dots, J$ and otherwise $K, K' = 1, \dots, J$. The operators \hat{j}^2 and \hat{j}_\pm are defined by

$$\hat{j}^2 = -\hbar^2 \left(\frac{\partial^2}{\partial \gamma^2} + \cot \gamma \frac{\partial}{\partial \gamma} - \frac{K^2}{\sin^2 \gamma} \right) \quad (3.5a)$$

$$\hat{j}_\pm = -\hbar \left(\pm \frac{\partial}{\partial \gamma} - K \cot \gamma \right) \quad (3.5b)$$

and satisfy

$$\hat{j}^2 P_j^K(\cos \gamma) = \hbar^2 j(j+1) P_j^K(\cos \gamma) \quad (3.6a)$$

$$\hat{j}_\pm P_j^K(\cos \gamma) = \hbar \Lambda_{jK}^\pm P_j^{K\pm 1}(\cos \gamma) \quad (3.6b)$$

where $P_j^K(\cos \gamma)$ is the associated Legendre function. Note that \hat{j}^2 and \hat{j}_\pm are not the usual angular momentum operators; they operate only on the associated Legendre function.

The flux correlation function, and thus rate constant via its integral in eq 1.1, is carried out for each value of total angular momentum J , yielding $k_f(T)$, and the total rate constant is

$$k(T) = \sum_{J=0} (2J+1)k_f(T) \quad (3.7)$$

the $2J+1$ factor comes from the sum over M_J , the projection of total angular momentum on a space-fixed axis, on which the dynamics in free space does not depend. As discussed thoroughly in our previous work⁷ on the $Cl + H_2$ reaction, one actually needs to calculate $k_f(T)$ only at a modest number of widely spaced values of J and can interpolate quite accurately to carry out the above sum; the reader should see ref 7 for a more complete discussion of this.

B. The J -Shifting Approximation. The above section describes the exact treatment of total angular momentum $J > 0$, but there are approximate treatments that are often reasonably accurate. The simplest of these is the J -shifting approximation,²⁸ which assumes that rotational motion is separable from that of the other ($3N - 6$) degrees of freedom and furthermore that it is that of the rigid molecular system at some reference geometry (typically that of the transition state). In this case the rotational energy is simply a constant added to the $J = 0$ Hamiltonian, and one can readily show that the rate constant is given by

$$k(T) = k_{J=0}(T) Q_{\text{rot}}^{\dagger}(T) \quad (3.8)$$

where Q_{rot}^{\dagger} is the rotational partition function for the rigid molecular system at the reference geometry. If this is a symmetric top (or nearly so), then

$$Q_{\text{rot}}^{\dagger}(T) = \sum_{J=0} (2J+1) \sum_{K=-J}^J e^{-\beta E_{JK}^{\dagger}} \quad (3.9a)$$

where the rotational energy levels are

$$E_{JK}^{\dagger} = B^{\dagger}[J(J+1) - K^2] + C^{\dagger}K^2 \quad (3.9b)$$

B^{\dagger} and C^{\dagger} being the appropriate rotation constants ($B^{\dagger} = \hbar^2/2I_B^{\dagger}$, etc.). For the $F + H_2$ transition state we find $B^{\dagger} = 2.340 \text{ cm}^{-1}$ and $C^{\dagger} = 98.17 \text{ cm}^{-1}$.

With this approximation one thus only has to calculate $k_f(T)$ for $J = 0$ and then multiply by a rotational partition function, a great simplification compared to the exact treatment of $J > 0$.

C. Principal Axis Helicity Conserving Approximation. Since the J -shifting approximation takes into account rotational motion at only one reference geometry, it may give a poor result if the dynamics becomes more nonlocalized (as is typically the case for higher temperatures). A better approximation is therefore one that takes into account the coordinate dependence of the rotation constants, i.e., centrifugal distortion, while still neglecting Coriolis coupling (the $K \neq K'$ coupling in the exact Hamiltonian of section III.A). This is the helicity-conserving approximation (HCA),²⁹ and the best HCA is the one suggested by McCurdy and Miller,³⁰ which chooses the body-fixed axis (the component of total angular momentum about which is assumed to be conserved) as the most unique instantaneous principal axes (PA) of the molecular system. The Hamiltonian for this principal axis helicity-conserving approximation (PA/HCA) is

$$\hat{H}^{JK} = \hat{H}_0 + E_{\text{rot}}^{JK}(r, R, \gamma) \quad (3.10a)$$

where \hat{H}_0 is the $J = 0$ Hamiltonian,

$$\hat{H}_0 = -\frac{\hbar^2}{2\mu} \frac{\partial^2}{\partial R^2} - \frac{\hbar^2}{2m} \frac{\partial^2}{\partial r^2} - \hbar^2 \left(\frac{1}{2\mu R^2} + \frac{1}{2mr^2} \right) \left(\frac{\partial^2}{\partial \gamma^2} + \cot \gamma \frac{\partial}{\partial \gamma} \right) + V(r, R, \gamma) \quad (3.10b)$$

and $E_{\text{rot}}^{JK}(r, R, \gamma)$ is the rotational energy of a symmetric top (determined by geometry r, R, γ),

$$E_{\text{rot}}^{JK}(r, R, \gamma) = \frac{1}{2} [A(r, R, \gamma) + B(r, R, \gamma)] [J(J+1) - K^2] + C(r, R, \gamma) K^2 \quad (3.10c)$$

where A , B , and C are given in terms of the principal moments of inertia in the usual way (i.e., $A = \hbar^2/2I_A$, etc.). For the present three-atom system these moments of inertia are

$$I_C(r, R, \gamma) = \frac{1}{2} (\mu R^2 + mr^2) - \frac{1}{2} [(\mu R^2)^2 + (mr^2)^2 + 2\mu R^2 mr^2 \cos 2\gamma]^{1/2} \quad (3.11a)$$

$$I_B(r, R, \gamma) = \frac{1}{2} (\mu R^2 + mr^2) + \frac{1}{2} [(\mu R^2)^2 + (mr^2)^2 + 2\mu R^2 mr^2 \cos 2\gamma]^{1/2} \quad (3.11b)$$

$$I_A(r, R, \gamma) = I_B + I_C = \mu R^2 + mr^2 \quad (3.11c)$$

$E_{\text{rot}}^{JK}(r, R, \gamma)$ is thus essentially a centrifugal potential that adds to the $J = 0$ Hamiltonian, eq 3.10b. This approximation has been rediscovered more recently by Bowman³¹ (termed by him the “adiabatic rotation approximation”) and used quite successfully for determining energies of bound and metastable states of the HCO system and has also been applied successfully by us⁷ in the thermal rate constant calculation for $Cl + H_2$ reaction.

One must thus carry out calculations of the rate constant $k_{JK}(T)$ with the Hamiltonian of eq 3.10a for at least a modest number of (J, K) values—each of which is essentially the difficulty of the $J = 0$ calculation—and then the total rate constant is

$$k(T) = \sum_{J=0} (2J+1) \sum_K k_{JK}(T) \quad (3.12)$$

As before, the J and K dependence of $k_{JK}(T)$ is usually sufficiently simple that one can interpolate a small number of (J, K) values quite well in order to carry out the sum in eq 3.12.

D. Basis Set. A discrete variable representation (DVR)^{32–34} has been used as the basis set to represent the Hamiltonian of the $F + H_2$ system. Specifically, for the radial degrees of freedom (i.e., R and r), the sinc-function DVR developed by Colbert and Miller³⁴ is used. For the angular degree of freedom, associated Legendre polynomials are chosen as a finite basis representation (FBR) and then transformed to a DVR in the usual way. To make the transformation simple, we discretize these associated Legendre polynomials using Gauss–Legendre quadrature (using more quadrature points than continuous functions), as done previously.⁷ The DVR is then generated by applying the corresponding rectangular transformation matrix.

The parameters N_B , N_γ , V_{cut} , and R_{max} serve to define the basis set. The radial sinc-function DVR has evenly spaced points with the grid spacing Δx related to the maximum kinetic energy in the problem. The grid constant, N_B , specifies the

number of points per thermal de Broglie wavelength for the radial coordinates:

$$\Delta x = \frac{2\pi}{N_B} \left(\frac{2\mu k_B T}{\hbar^2} \right)^{-1/2} \quad (3.13)$$

For the $F + H_2$ reaction we find $N_B = 16$ –26 yields converged results; this is somewhat larger than we have found for other reactions due to the large exoergicity. The number of DVR points for the angular coordinate is given by N_γ . For the $J = 0$ and PA/HCA calculation, N_γ is taken to be 14–16, whereas for the exact calculation of $J > 0$ case, N_γ is taken to be 20.

The DVR basis is determined by first laying down a “raw” grid in the Jacobi coordinates of the $F + H_2$ arrangement, which is then truncated by three criteria. (1) An energy cutoff is used: if the potential energy at a DVR point is greater than V_{cut} , the point is discarded (here $V_{\text{cut}} \approx 1.3$ –1.8 eV); (2) in the asymptotic valleys of the reactant and product arrangements points with $s > 4$ au or $s < -4$ au are neglected, where $s = r_{H-H} - r_{F-H} + X$ and $1.6 \text{ au} < X < 2.6 \text{ au}$ define the flux dividing surface as discussed in section III.F; and (3) the first n points in the R -grid are discarded. This is possible because insertion of F into the H_2 bond is not allowed by the potential energy surface, n is a convergence parameter in the calculations, typically taken to be 4 or 5.

E. Time Propagation. Due to the large exoergicity of the $F + H_2$ reaction, it is necessary to use very accurate propagators. In our calculation, we applied the Chebyshev propagator³⁵ for the imaginary time (i.e., the Boltzmann operator) propagation, and the sixth-order symplectic integrator³⁶ for the real time propagation. Both of these are of higher order than the split operator³⁷ and thus can achieve more accurate results with moderate numerical effort. Furthermore, these two propagators are easily implemented, with the primary computational task being the Hamiltonian matrix acting on a vector. This is particularly convenient for the exact $J > 0$ rate calculation, since from eq 3.4 the Hamiltonian matrix has a simple block tridiagonal structure, and thus its operation on a vector scales linearly versus the maximum angular momentum projection onto the body-fixed axis, K_{max} . In the previous split-operator propagation for $Cl + H_2$ reaction,⁷ each (j, K) block had to be diagonalized, and thus the propagator for angular degree of freedom was dense and scaled quadratically in K_{max} . For the $F + H_2$ reaction, we found that $K_{\text{max}} = 4$ was adequate to obtain converged results, so that the symplectic integrator is much more efficient than the split-operator.

F. Flux Operator and Dividing Surface. The form for the flux operator used in this work is

$$\hat{F} = \frac{i}{\hbar} [\hat{H}, \hat{h}(s(\mathbf{q}))] \quad (3.14)$$

where the dividing surface separating reactants and products is defined by the equation $s(\mathbf{q}) = 0$ and $h(s)$ is the Heaviside step function, which is zero for $s < 0$ and 1 for $s > 0$. This is not the only possible expression for \hat{F} , and the different choices do not all possess the same numerical properties in a finite basis representation. This form, however, is most easily incorporated in a multidimensional problem and can be conveniently applied using sparse matrix multiplication techniques.

The matrix elements of the flux operator in the DVR are easily evaluated as

$$F_{jj'} = \frac{i}{\hbar} T_{jj'} [h(s_{j'}) - h(s_j)] \quad (3.15)$$

where $h(s_j)$ is the step function evaluated at the j th DVR point, and $T_{jj'}$ is the kinetic energy matrix. The dividing surface used in this study is defined by $s = R - X = 0$, where X is taken to be between 4.0 and 5.0 au. We note that the exoergicity of this reaction dictates that the flux dividing surface be moved somewhat into the reactant valley for the reasons given in section II for the splitting up of the Boltzmannized flux operator.

G. Absorbing Potential. The absorbing potential is taken to be a quartic function of the coordinate s defined in section III.D:

$$\epsilon(s) = \lambda \left(\frac{s - s_0}{s_{\text{max}} - s_0} \right)^4 \quad (3.16)$$

We have found this form works well and is easy to converge with respect to the parameters λ , s_0 , and s_{max} . Typically $\lambda = 1.5$ –2.0 eV and s_0 is chosen such that approximately 30–40% of the grid points are in absorbing region.

IV. Results and Discussion

Calculations of the thermal rate constants for the $F + H_2 \rightarrow HF + H$ reaction have been carried out using the methodology described in sections II and III over the temperature range 300–700 K. The exact treatment of the $J > 0$ contribution (section III.A) was carried out at two temperatures (300 and 600 K) in order to calibrate the simpler JSA (section III.B) and PA/HCA (section III.C) approaches that were then used for more values of T . As usual,³⁸ the rate constant given by eq 1.1 was also divided by the factor,

$$q_{\text{el}}(T) = 2 + e^{-\Delta/k_B T} \quad (4.1)$$

which arises from the ratio of electronic partition functions, where $\Delta = 404 \text{ cm}^{-1}$ is the spin–orbit splitting^{39,40} of $F(^2P_J)$. The rate constants presented here are numerically converged to at least $\sim 10\%$. The accuracy is primarily limited by the exoergicity of the reaction; it could be improved by significantly increasing the density of DVR grid points (i.e., increasing N_B) with a corresponding cost in the calculation time.

Figure 2 shows the even and odd parity $J = 0$ flux–flux autocorrelation functions for the reaction at (a) $T = 300 \text{ K}$ and (b) $T = 600 \text{ K}$. They were obtained by propagating 10 and 12 eigenvectors, respectively, of the half-Boltzmannized flux operator (while the size of the DVR basis was 1800 and 2000 grid points, respectively). For both temperatures the propagation time must be rather long in order to capture the slowly decaying, long time tail of the correlation function. The even parity correlation function converges to zero in $\sim 325 \text{ fs}$ at 300 K and in $\sim 90 \text{ fs}$ at 600 K. Note that in both cases the odd parity correlation function decays to zero significantly faster (in ~ 175 and ~ 50 for 300 and 600 K, respectively). As discussed above, the flux dividing surface is placed somewhat into the reactant valley, and thus amplitude reflected from the barrier (even amplitude that never reaches the transition state and is therefore not transition state theory “violating”) recrosses the dividing surface.

It is worth noting from Figure 2 that the odd and even parity rates will obviously be quite different. This is in contrast to the $Cl + H_2$ reaction,⁷ which has a large barrier for internal rotation of H_2 in the transition state and thus has equal rates for even and odd parity. This is a reflection of the fact that the barrier to internal rotation of H_2 at the $F \cdots H_2$ transition state is quite small.

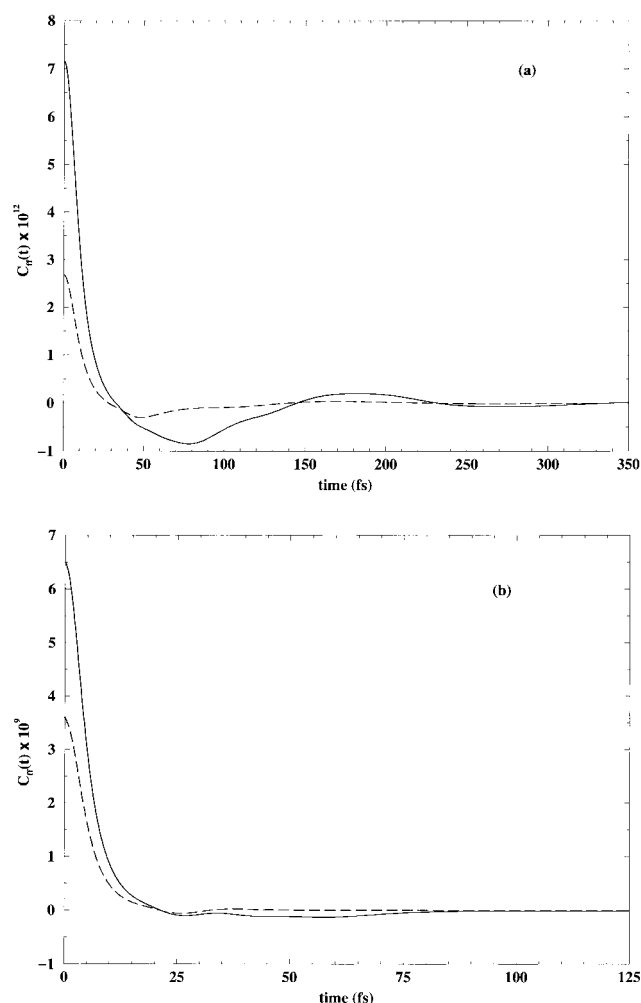


Figure 2. Even (solid line) and odd (dashed line) parity flux-flux autocorrelation functions for the $F + H_2$ reaction at (a) $T = 300$ K and (b) $T = 600$ K.

TABLE 1: Comparison of Thermal Rate Constants from Exact $J \neq 0$ Calculations with Those Using the PA/HCA and J -Shifting Approximations to Include the Effect of $J \neq 0$ Total Angular Momentum for the Three-Dimensional $F + H_2$ Reaction in Units of $\text{cm}^3 \text{ molecule}^{-1} \text{ s}^{-1}$

temp (K)	$k(T)/10^{-13}$		
	J -shifting	PA/HCA	exact
300	2.52	1.93	2.26
350	3.48	2.58	
400	4.42	3.27	
450	5.08	3.74	
500	5.74	4.16	
600	7.32	5.27	5.68
700	8.62	6.19	

Table 1 compares the total rate constants from the exact $J \neq 0$ calculation with those obtained using the simpler JSA and PA/HCA approaches. Note that the JSA rate constants are greater than the exact rates, while the PA/HCA gives values that are lower. Overall, the agreement is reasonably good, particularly for the PA/HCA rates, which are within 15% of the exact rate at 300 K and within 8% at 600 K. The J -shifting rates are within 12 and 30% of the exact result at 300 and 600 K, respectively. The accuracy of these approximate approaches underscores their usefulness, especially when one considers the large savings in computational effort they provide. An interesting feature of the rates presented here is that we observe a very weak dependence of the $J = 0$ rate constant on the temperature.

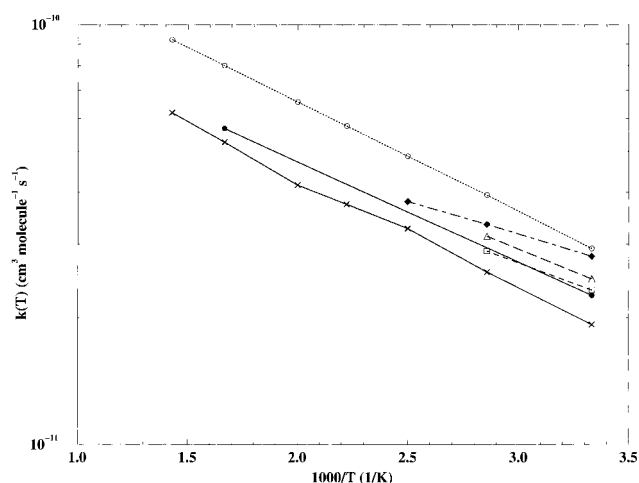


Figure 3. Arrhenius plot of the thermal rate constant for the $F + H_2$ reaction. The present exact results are shown by the solid line with solid circles, the present PA/HCA results by the solid line with \times 's, the theoretical results of Rosenman et al. by the dot-dashed line and solid diamonds, the experimental results of Wurzburg and Houston by the dashed line and open squares, the experimental results of Stevens et al. by the long dashed line and open triangles, and the experimental results of Heidner et al. by the dotted line and open circles. (The lines are intended simply as a guide to the eye.)

In fact, the $J = 0$ rate is seen to *decrease* above 400 K. However, the total rate constant increases with increasing temperature. Thus, the qualitative Arrhenius behavior of the total rate is dominated by the effects of overall rotation.

Several other dynamics calculations have been carried out on this same Stark–Werner (SW) surface, including quasiclassical trajectory⁴¹ and quantum scattering studies.⁴² We refer the reader to the recent excellent review by Manolopoulos²² on this reaction. Of particular interest in the context of this paper are the calculations by Rosenman et al.³⁸ They calculated reactive cross sections and thermal rate constants on the SW surface using the helicity-conserving approximation (HCA) to include nonzero total angular momentum. They obtained results in reasonably good agreement with the experimentally measured rates of Wurzburg and Houston⁴³ and Stevens et al.⁴⁴ Another experimental study by Heidner et al.⁴⁵ has reported rate constants that are $\sim 20\%$ larger than the two experiments just mentioned, but agree very well with the calculations of Rosenman et al.³⁸ at $T = 298$ K.

There are, however, some questions in applying the conventional HCA—which uses the \mathbf{R} axis as the body-fixed axis—to this reaction since \mathbf{R} is not a very good “almost” symmetric top axis for this molecular system. Indeed, we found in our previous study⁷ of the similar reaction $Cl + H_2 \rightarrow HCl + H$ that the conventional HCA overestimated the rates by ~ 20 – 40% , a result even worse than the simple J -shifting approximation. The PA/HCA, which uses one of the instantaneous principal axes as the body-fixed axis for the purpose of making the helicity-conserving approximation, is thus preferred.

Figure 3 is an Arrhenius plot of the present results compared with those from previous experiments^{43–45} and theoretical calculations.³⁸ The numerical values of the rates are given in Table 2. The conventional HCA rates by Rosenman et al.³⁸ are larger (by $\sim 30\%$) at all temperatures than the present exact treatment of the $J > 0$ case, indicating that HCA is poorer than PA/HCA or even simple J -shifting approximation and is thus not as useful an approximation for treating this reaction.

The rate constants obtained from the exact treatment of the $J > 0$ case described in this paper are in excellent agreement

TABLE 2: Experimental and Theoretical Total Thermal Rate Constants for the Three-Dimensional F + H₂ Reaction in Units of cm³ molecule⁻¹ s⁻¹

temp (K)	$k(T)/10^{-11}$				
	WH ^a	SBA ^b	HBGM ^c	RHPB ^d	present
298	2.33	2.48	2.93	2.81	2.26 ^e
350	2.89	3.14	3.94	3.35	
400			4.88	3.80	
450			5.76		
500			6.57		
600			8.01		5.68
700			9.23		

^a Wurzberg and Houston; ref 43. ^b Stevens, Brune, and Anderson; ref 44. ^c Heidner, Bott, Gardner, and Melzer; ref 45. ^d Rosenman, Hochman-Kowal, Persky, and Baer; ref 38. ^e 300 K.

(within 10%) with the experimental results of both Wurzberg and Houston⁴³ and Stevens et al.⁴⁴ The rate constants experimentally measured by Heidner et al.⁴⁵ are larger than all the other reported rates, including those presented here at both 300 and 600 K. Unfortunately, above 400 K these are the only experimental rates that have been reported to our knowledge. It would be beneficial to have more experimental data at higher temperatures to resolve such discrepancies and to allow more definite conclusions on the quality of the potential energy surface.

V. Concluding Remarks

The flux-flux autocorrelation function methodology has been used successfully to calculate thermal rate constants for the F + H₂ reaction "directly". Because of the extreme exothermicity of this reaction, a variation of our previous version of the calculation has proved very useful.

The contribution to the rate for total angular momentum $J > 0$ was treated both exactly (at two temperatures) and also via the J -shifting and principal axis helicity-conserving approximations. The latter approximation is the better (good to 8–15%), but the former (good to 12–30%) is simpler.

Good agreement is obtained with the experimental results of Wurzberg and Houston⁴³ and Stevens et al.⁴⁴ at $T = 300$ K. There is, however, a caveat with regard to this good agreement: ⁴⁶ as Manolopoulos discusses,²² it is expected that the inclusion of spin-orbit coupling in the potential energy surface will raise the effective classical barrier height (by lowering the F + H₂ asymptote) by ~ 0.3 – 0.4 kcal/mol ($\sim 1/3$ of the spin-orbit splitting in the F atom), and this will tend to decrease the rate constant. If, on the other hand, electronically nonadiabatic dynamics is taken into account, then nonadiabatic transitions from the nonadiabatic potential surfaces will tend to increase the rate. Thus an absolutely definitive calculation of the rate constant, which could be carried out by the present methodology, must await potential energy surfaces and dynamical treatments that include these effects.

Acknowledgment. The authors would like to thank Prof. David E. Manolopoulos for providing us with the potential energy surface and the $J = 0$ cumulative reaction probabilities of Castillo et al.⁴² They also wish to acknowledge Dr. Timothy C. Germann and David E. Skinner for useful discussions. This work was supported by the Director, Office of Energy Research, Office of Basic Energy Sciences, Chemical Sciences Division of the U.S. Department of Energy under Contract No. DE-AC03-76SF00098, by the Laboratory Directed Research and Development (LDRD) project from National Energy Research Scientific Computing (NERSC) Center, Lawrence Berkeley National

Laboratory, and also by National Science Foundation Grant No. CHE 94-22559.

References and Notes

- (1) (a) Miller, W. H. In *Dynamics of Molecules and Chemical Reactions*; Zhang, Z. J., Wyatt, R., Eds.; Marcel Dekker: New York, 1996; p 389. (b) Miller, W. H. *J. Phys. Chem.* **1998**, *102*, 793.
- (2) Miller, W. H. *J. Chem. Phys.* **1974**, *61*, 1823.
- (3) Miller, W. H.; Schwartz, S. D.; Tromp, J. W. *J. Chem. Phys.* **1983**, *79*, 4889.
- (4) See also: Yamamoto, T. *J. Chem. Phys.* **1960**, *33*, 281.
- (5) Thompson, W. H. In *Highly Excited Molecules: Relaxation, Reaction and Structure*; ACS Symposium Series 678; Mullin, A. S., Schatz, G. C., Eds.; American Chemical Society: Washington, DC, 1997.
- (6) Thompson, W. H.; Miller, W. H. *J. Chem. Phys.* **1997**, *106*, 142; **1997**, *107*, 2164 (E).
- (7) Wang, H.; Thompson, W. H.; Miller, W. H. *J. Chem. Phys.* **1997**, *107*, 7194.
- (8) Lanczos, C. *J. Res. Natl. Bur. Stand.* **1950**, *45*, 255.
- (9) Saad, Y. *Numerical Methods for Large Eigenvalue Problems*; Halstead Press: New York, 1992.
- (10) Goldberg, A.; Shore, B. W. *J. Phys. B* **1978**, *11*, 3339.
- (11) Leforestier, C.; Wyatt, R. E. *J. Chem. Phys.* **1983**, *78*, 2334.
- (12) Kosloff, R.; Kosloff, D. *J. Comput. Phys.* **1986**, *63*, 363.
- (13) Neuhauser, D.; Baer, M. *J. Chem. Phys.* **1989**, *90*, 4351. Neuhauser, D.; Baer, M. *J. Chem. Phys.* **1989**, *91*, 4651. Neuhauser, D.; Baer, M.; Kouri, D. J. *J. Chem. Phys.* **1990**, *93*, 2499.
- (14) Jolicard, G.; Austin, E. J. *J. Chem. Phys. Lett.* **1985**, *121*, 106. Jolicard, G.; Austin, E. J. *J. Chem. Phys.* **1986**, *103*, 295. Jolicard, G.; Perrin, M. Y. *J. Chem. Phys.* **1987**, *116*, 1. Jolicard, G.; Leforestier, C.; Austin, E. J. *J. Chem. Phys.* **1988**, *88*, 1026.
- (15) Last, I.; Neuhauser, D.; Baer, M. *J. Chem. Phys.* **1992**, *96*, 2017. Last, I.; Baer, M. *J. Chem. Phys. Lett.* **1992**, *189*, 84. Last, I.; Baram, A.; Baer, M. *J. Chem. Phys. Lett.* **1992**, *195*, 435. Last, I.; Baram, A.; Szichman, H.; Baer, M. *J. Phys. Chem.* **1993**, *97*, 7040.
- (16) Seideman, T.; Miller, W. H. *J. Chem. Phys.* **1992**, *96*, 4412. Seideman, T.; Miller, W. H. *J. Chem. Phys.* **1992**, *97*, 2499. Miller, W. H.; Seideman, T. In *Time Dependent Quantum Molecular Dynamics: Experiment and Theory*; Broeckhove, J., Ed.; NATO ARW, 1992.
- (17) Germann, T. C.; Miller, W. H. *J. Phys. Chem.* **1997**, *101*, 6358.
- (18) (a) Park, T. J.; Light, J. C. *J. Chem. Phys.* **1988**, *88*, 4897. (b) Brown, D.; Light, J. C. *J. Chem. Phys.* **1992**, *97*, 5465.
- (19) Manthe, U. *J. Chem. Phys.* **1995**, *102*, 9205.
- (20) Stark, K.; Werner, H. J. *J. Chem. Phys.* **1996**, *104*, 6515.
- (21) Weaver, A.; Metz, R. B.; Bradforth, S. E.; Neumark, D. M. *J. Chem. Phys.* **1990**, *93*, 5352. Weaver, A.; Neumark, D. M. *Faraday Discuss. Chem. Soc.* **1991**, *91*, 5. Bradforth, S. E.; Arnold, D. W.; Neumark, D. M.; Manolopoulos, D. E. *J. Chem. Phys.* **1993**, *99*, 6345.
- (22) Manolopoulos, D. E. *J. Chem. Soc., Faraday Trans.* **1997**, *93*, 673.
- (23) Manolopoulos, D. E.; Stark, K.; Werner, H. J.; Arnold, D. W.; Bradforth, S. E.; Neumark, D. M. *Science* **1993**, *262*, 1852.
- (24) For one dimension there are only two nonzero eigenvalues of $\hat{F}(\beta)$, the eigenvectors of which are complex conjugates of each other.
- (25) Miller, W. H. *J. Chem. Phys.* **1968**, *49*, 2373.
- (26) Rose, M. E. *Elementary Theory of Angular Momentum*; John Wiley & Sons, Inc.: New York, 1967.
- (27) Choi, S. E.; Light, J. C. *J. Chem. Phys.* **1990**, *92*, 2129. The phase convention we adopt is different from this paper. Therefore as shown in the text, we use the complex conjugate of Wigner function as "ket".
- (28) Bowman, J. M. *J. Phys. Chem.* **1991**, *95*, 4960.
- (29) Pack, R. T. *J. Chem. Phys.* **1974**, *60*, 633.
- (30) McCurdy, C. W.; Miller, W. H. *ACS Symposium Series No. 56*; Brooks, P. R.; Hayes, E. F., Eds.; American Chemical Society: Washington, DC, 1977; pp 239–242.
- (31) (a) Bowman, J. M. *J. Chem. Phys. Lett.* **1994**, *217*, 36; (b) Qi, J.; Bowman, J. M. *J. Chem. Phys.* **1996**, *105*, 9884.
- (32) Harris, D. O.; Engerholm, G. G.; Gwinn, W. D. *J. Chem. Phys.* **1965**, *43*, 1515.
- (33) Lill, J. V.; Parker, G. A.; Light, J. C. *J. Chem. Phys. Lett.* **1982**, *89*, 483. Light, J. C.; Hamilton, I. P.; Lill, J. V. *J. Chem. Phys.* **1985**, *82*, 1400. Bačić, Z.; Light, J. C. *J. Chem. Phys.* **1986**, *85*, 4594. Whitnell, R. M.; Light, J. C. *J. Chem. Phys.* **1988**, *89*, 3674.
- (34) Colbert, D. T.; Miller, W. H. *J. Chem. Phys.* **1992**, *96*, 1982.
- (35) Tal-Ezer, H.; Kosloff, R. *J. Chem. Phys.* **1984**, *81*, 3967.
- (36) Gray, S. K.; Manolopoulos, D. E. *J. Chem. Phys.* **1996**, *104*, 7099.
- (37) Feit, M. D.; Fleck, Jr., J. A.; Steiger, A. *J. Comput. Phys.* **1982**, *47*, 412.
- (38) Rosenman, E.; Hochman-Kowal, S.; Persky, A.; Baer, M. *J. Chem. Phys. Lett.* **1996**, *257*, 421.
- (39) Trnřlar, D. G. *J. Chem. Phys.* **1972**, *56*, 3189.
- (40) Muckerman, J. T.; Newton, M. D. *J. Chem. Phys.* **1972**, *56*, 3191.

- (41) Aoiz, F. J.; Bañares, L.; Herrero, V. J.; Sáez Rábanos, V.; Stark, K.; Werner, H. J. *Chem. Phys. Lett.* **1994**, 223, 215. Aoiz, F. J.; Bañares, L.; Herrero, V. J.; Sáez Rábanos, V.; Stark, K.; Werner, H. J. *J. Chem. Phys.* **1994**, 98, 10665. Aoiz, F. J.; Bañares, L.; Herrero, V. J.; Sáez Rábanos, V.; Stark, K.; Werner, H. J. *J. Chem. Phys.* **1995**, 102, 9248.
- (42) Castillo, J. F.; Manolopoulos, D. E.; Stark, K.; Werner, H. J. *J. Chem. Phys.* **1996**, 104, 6531.

- (43) Wurzburg, E.; Houston, P. L. *J. Chem. Phys.* **1980**, 72, 4811.
- (44) Stevens, P. S.; Brune, W. H.; Anderson, J. G. *J. Phys. Chem.* **1989**, 93, 4068.
- (45) Heidner, III, R. F.; Bott, J. F.; Gardner, C. E.; Melzer, J. E. *J. Chem. Phys.* **1980**, 72, 4815.
- (46) We thank the referee for suggesting that these issues be noted.